AGU100 ADVANCING EARTH AND SPACE SCIENCE

JGR

Journal of Geophysical Research: Biogeosciences

RESEARCH ARTICLE
10.1029/2018JG004726

Key Points:
- Prior to rainfall, cyanobacterial soil crusts have higher soil surface roughness (SSR) than physical crusts
- SSR of physical soil crusts is highly responsive to low rainfall; SSR of cyanobacterial soil crusts is stable in response to low rainfall
- Splash loss is associated with topographic roughness and spatial patterning

Correspondence to:
J. E. Bullard,
j.e.bullard@lboro.ac.uk

Citation:
Bullard, J. E., Ockelford, A., Strong, C., & Aubault, H. (2018). Effects of cyanobacterial soil crusts on surface roughness and splash erosion. *Journal of Geophysical Research: Biogeosciences*, *123*, 3697–3712. https://doi.org/10.1029/2018JG004726

Received 31 JUL 2018
Accepted 26 NOV 2018
Accepted article online 6 DEC 2018
Published online 27 DEC 2018

Effects of Cyanobacterial Soil Crusts on Surface Roughness and Splash Erosion

Joanna E. Bullard[1], Annie Ockelford[2], Craig Strong[3], and Helene Aubault[1]

[1]Geography and Environment, Loughborough University, Loughborough, UK, [2]School of Environment and Technology, University of Brighton, Brighton, UK, [3]Fenner School for Environment and Society, Australian National University, Canberra, ACT, Australia

Abstract Soil surface roughness (SSR) modifies interactions and feedback processes between terrestrial and atmospheric systems driven by both the abiotic and biotic components of soils. This paper compares SSR response to a low-intensity multiday rainfall event for soils with and without early successional stage cyanobacteria-dominated biological soil crusts (CBCs). A rainfall simulator was used to apply 2, 5, and 2 mm of rain separated by a 24-hr period over 3 days at an intensity of 60 mm/hr. Changes in SSR were quantified using geostatistically derived indicators calculated from semivariogram analysis of high-resolution laser scans. The CBCs were stronger and splash erosion substantially less than from the physical soil crusts. Prior to rainfall treatment, soils with CBCs had greater SSR than those without. The rainfall treatments caused the physical crusted soils to increase SSR and spatial patterning due to the translocation of particles, soil loss, and the development of raindrop impact craters. Rainfall caused swelling of cyanobacterial filaments but only a slight increase in SSR, and raindrop impact cratering and splash loss were low on the soils with CBCs. There is no relationship between random roughness and splash erosion, but an increase in splash loss was associated with an increase in topographic roughness and small-scale spatial patterning. A comparison of this study with other research indicates that for rainfall events up to 100 mm, the effectiveness of CBCs in reducing soil loss is >80% regardless of the rainfall amount and intensity, which highlights their importance for landscape stabilization.

Plain Language Summary Human and ecological systems rely on soils for the provision of water and nutrients, to support plant growth, for regulation of the water cycle and for the storage of carbon. The stability of soil surfaces can be controlled by the presence of *crusts*. Physical crusts form in the response to rainfall events causing the soil to break down and compact. Biological soil crusts are formed when cyanobacteria, fungi, algae, lichens, and mosses grow and bind the soil together. Biological soil crusts are particularly important in arid and semiarid areas where they cover up to 70% of interplant spaces. However, little is known about how the crusts control infiltration, runoff, and soil erosion rates or which is more effective at stabilizing the soil surface. In this study we use high-resolution laser scanning to characterize how the stability of the soil surface is controlled by both physical and biological crusts in response to different rainfall events. We discuss the differences in the between the two crusts and observe that biological soil crusts can reduce soil loss by greater than 80% regardless of the rainfall amount and intensity which highlights their importance for landscape stabilization.

1. Introduction

Soil surface microtopography plays an important role in modifying interactions and feedback processes between terrestrial and atmospheric systems at a range of scales (Cammeraat, 2002; Martin et al., 2008; Rodríguez-Caballero et al., 2012; Smith, 2014). It can also affect the susceptibility of soils to erosion by both water (e.g., Kirkby, 2002; Luo et al., 2018) and wind (e.g., Chappell et al., 2006; Zobeck & Popham, 1997). In this paper the term soil surface roughness (SSR) is used to encompass soil surface morphology, spatial patterning, and microtopography (Römkens & Wang, 1986). The focus is on microrelief at the centimeter scale controlled by primary soil particles (≤mm), the size and organization of soil aggregates (mm), and the presence of physical and biological crusts. Feedback relationships between hydrological regime and SSR at this scale are driven by both the abiotic (e.g., Le Bissonais 1996a, 1996b) and biotic (Belnap, 2006; Ferrenberg et al., 2017; Rodríguez-Caballero et al., 2013) components of soils.

Soil particle size and aggregation are key determinants of abiotic SSR. Interparticle or microtopographic depressions can retain water causing ponding as well as acting as interception niches that trap particles dislodged by raindrop-driven splash erosion (Abrahams et al., 2001; Carmi & Berliner, 2008; Kinnell, 2005). This can change runoff rates and overland flow (Antoine et al., 2009; Darboux et al., 2002; Helming et al., 1998; Kamphorst et al., 2000). SSR at small scales is highly dynamic in response to raindrop impact as the soil structural units are broken down from macroaggregates (>250 μm) to microaggregates (20–250 μm) to primary soil particles (Emerson & Greenland, 1990; Le Bissonais, 1996a, 1996b; Le Bissonais et al., 2005). This breakdown of structural units often results in the formation of physical soil crusts comprising a thin surface layer a few millimeters thick that is more dense and with a lower porosity than the underlying soil (Assouline, 2004). Although the vertical surface change may only be of the order of 1–2 mm, these microrelief dynamics can affect hydrological regime by binding particles together and reducing rates of infiltration and splash erosion, but increasing surface runoff and sediment yield (e.g., Agassi et al., 1985; Bradford & Huang, 1993; Morin et al., 1989). Crust formation and resultant resistance of the soil to erosion is substantially controlled by soil texture (e.g., Bedaiwy, 2008), structure (e.g., Farres, 1978) and the frequency, intensity, and duration of rainfall events (Fan et al., 2008; Nciizah & Wakindiki, 2014). Surface sealing and ponding during physical crust formation typically reduces SSR (e.g., Croft et al., 2013; Vermang et al., 2013), although on fine soils under low rainfall the creation of raindrop impact craters may cause an increase in surface roughness (Bullard et al., 2018).

SSR at this millimeter-scale can also be affected by biotic factors such as biological soil crusts (BSCs). BSCs are formed by cyanobacteria, fungi, algae, lichens, and mosses on the soil surface, and highly developed BSCs (typically lichen- or moss-dominated) create rougher soil surfaces than those in the early stages of successional development (cyanobacteria-dominated) (Belnap, 2006; Chamizo, Cantón, Lázaro, et al., 2012). Kidron (2007) suggested that runoff would be highest from young cyanobacterial crusts that are sufficient to decrease soil infiltration rates but are still smooth, whereas runoff from more mature, rougher crusts may be reduced (Rodríguez-Caballero et al., 2012). The relationships among BSC successional stage, infiltration rates, runoff, soil loss, and microtopography are highly complex and can vary according to factors such as soil texture and rainfall intensity and duration (Chamizo et al., 2013; Rodríguez-Caballero et al., 2013). For example, although Kidron et al. (2012) suggest enhanced microtopography caused by BSC formation on fine-textured soils controls infiltration rates, microtopographic effects are likely to be negligible under high-intensity rain because microdepressions will be rapidly filled leading to runoff generation (Rodríguez-Caballero et al., 2012). An additional contributor to SSR on soils with biological crusts is the swelling response of the organisms to wetting. BSCs absorb water readily and have a very rapid growth response to rainfall (Strong et al., 2013). As they absorb water, the volume of the BSC increases, modifying surface microtopography and increasing SSR (Rodríguez-Caballero et al., 2015; Wang et al., 2017).

BSCs can cover up to 70% of interplant spaces in arid and semiarid regions (Belnap et al., 2005), but the soil surface often comprises a mosaic of small patches (mm-cm) some with BSCs present and others without. It is difficult to separate the direct and indirect effects of physical crust development and biological soil crust development on SSR and soil hydrological properties (Rodríguez-Caballero et al., 2012; Rossi et al., 2012) but excluding raindrop impact cratering, during a rainfall event the SSR of soils without BSCs could be expected to decrease due to aggregate disintegration and physical crust formation, while the SSR of soils with early successional stage BSCs might be expected to increase due to water absorption and organism growth. Where low-magnitude rain events are insufficient to cause ponding and the surface sediments are not sealed or form a sieving crust, raindrop impact cratering can occur and increase SSR (Bullard et al., 2018; Rajot et al., 2003).

The aim of this paper is to compare surface roughness response to a low-intensity multiday rainfall event for two soils with and without early successional stage, cyanobacteria-dominated biological soil crusts. Both soils are from a dryland region and have only very fine aggregates (<1.4 mm) present but are susceptible to both physical and biological crusting. A rainfall simulator is used to create a multiday event typical of many dryland regions, which is low magnitude (<10 mm) but of relatively high frequency (several times a year) and therefore likely to result in SSR that persists for days-months if undisturbed. High-resolution laser scans are used to quantify changes in SSR during the event and analyzed using a geostatistical approach. The specific objectives are for the two soils with/without cyanobacterial crusts (i) to compare soil loss by rainsplash, infiltration rates, and surface crust strength; (ii) to quantify changes to soil surface roughness in response to rainfall; and (iii) to determine any relationships between soil loss and SSR. Experiments were not replicated, which

Table 1
Locations and Characteristics of Soil Samples

Sample	Latitude	Longitude	Salinity (μS)	LOI (%)	Soil type	Degree of dispersion	Percent clay	Percent silt	Percent sand
Soil A	−23.7622	140.9948	101.2	1.06	Sandy loam	MD	6.38	45.19	48.43
						ID	12.21	39.32	48.48
Soil B	−23.7676	140.9951	117.2	0.91	Loamy fine sand	MD	3.85	19.75	76.41
						ID	12.63	28.96	58.42

Note. LOI = loss on ignition; MD = minimal dispersion; ID = intermediate dispersion. See text for details.

precludes any statistical comparison of responses; however, the differences are described and raise some interesting research questions for future investigation.

2. Methods

2.1. Soil Characteristics

Experiments were conducted on two different soils collected from the Lake Constance claypan, Diamantina Lakes, which is located in eastern Australia. The geomorphic context of the site is described in detail by McTainsh et al. (1999) and Chappell et al. (2007). Soil A is a sandy loam, Soil B is a loamy fine sand, and both comprise individual particles and fine aggregates <1.4-mm diameter (Table 1). Analysis of the genetic material in the soils shows that the biota of both soils are dominated by cyanobacteria (28%), of which the dominant cyanobacterial genus is *Phormidium (20%–23%)*, followed by *Microcoleus* sp., which is more abundant in soil B (2.1%) than soil A (0.2%; D. Elliott personal communication, July 2018). The total microbial assemblage results in a natural biotic component for both soils that forms a thin, light cyanobacterial soil crust (class 1 in Belnap et al., 2008). Particle size analysis of the soils was undertaken using a Beckman Coulter LS280 laser sizer in the range 0.375–1,000 μm with 85 class intervals. Particle size distributions were calculated for minimally dispersed (MD) and intermediately dispersed (full mechanical-dispersion, no chemical dispersion: ID) soils following the protocols of Mason et al. (2003, 2011) as described by Bullard et al. (2018). Full disaggregation (including sonication and chemical dispersion) was not performed for this paper. Soil salinity prior to experimentation was determined using electrconductivity (TPS MC-80 pH-mV-Temp Meter; Rayment & Higginson, 1992). Soil organic matter was determined using loss on ignition.

For the control experiments without cyanobacterial crusts subsamples of the soils were sterilized at 100 °C for 24 hr to destroy any viable organic material. These soils are referred to as *physical* (labeled A_{PHYS} and B_{PHYS}) and were packed into trays 200 × 140 × 50 mm filled to the surface and lightly compacted. For each soil, three trays were prepared one of which was used for prerainfall infiltration measurements and two of which were subjected to rainfall treatments. Of the latter, one tray was used for destructive crust penetration resistance measurements and the other was used for nondestructive measurements (laser profiling) and postrainfall infiltration.

Figure 1. Cyanobacterial crust grown on soil B after 60 days at 2-mm rainfall per day. *Microcoleus* spp. filaments can clearly be seen on the soil surface. The width of the tray is 120 mm.

Cyanobacterial soil crusts (CBC) were grown on subsamples of each of the two soils (A_{CBC} and B_{CBC}). Trays 120 × 1,200 × 50 mm were filled with untreated soil that contained a natural population of biota, placed in a greenhouse for 60 days and lightly spray irrigated with filtered water to the equivalent of 2 mm of rainfall per day but at insufficient intensity to cause raindrop impacts. This enabled the natural organisms in the soil to grow and form a biological soil crust which was dominated by cyanobacteria (*Phormidium* spp. and *Microcoleus* spp.), and with minor components of algae and moss (Figure 1). Although the water supply was filtered and this was the only experiment being conducted in the greenhouse, it was not possible to completely isolate the trays in the greenhouse from other potential sources of microbes that may have affected the crust growth. Cyanobacterial crust growth was visually assessed based on soil surface

darkness and *greenness* (Belnap et al., 2008; Strong et al., 2013) to monitor growth. The soils with CBCs were dried for 11 days at 35 °C and 30% humidity to reduce soil moisture content to <5% prior to experimentation. Although the trays for biotic and abiotic soils were different sizes, the soil depth was the same in each case (50 mm) to ensure infiltration rates would not be differentially affected.

The removal of soils from their natural context and subsequent reconstitution in the laboratory is likely to disturb natural soil structures, and consequently, the response to rainfall impact may not be identical to that which would be observed if the experiments were conducted in situ. However, the removal of soils and their use in laboratory experiments is a very common approach for testing soil response to rainfall, splash erosion and for experiments using biological soil crusts because it allows certain other variables to be controlled, such as antecedent moisture (Fan et al., 2008; Feng et al., 2013; Gomez & Nearing, 2005; Hill et al., 2002). A large proportion of the work with which the results presented here are compared has taken this approach and has thus been subject to the same limitations. A particular difference in the experiments described in this paper is that the cyanobacterial crust was grown from the natural assemblage present in the soils rather than being grown from a culture, often restricted to a single species, and added to the soil (McKenna Neuman et al., 1996; O'Brien & McKenna Neuman, 2012Kheirfam et al., 2017).

2.2. Rainfall Simulation

The rainfall regime in the region of Australia from which the soils were obtained is typically characterized by 2–3 days of low rainfall (<6 mm/day) separated by long dry periods and with occasional low-frequency, high-magnitude rainfall events (Bullard et al., 2018; Connolly et al., 1998). For this study we focused on the impact of low-intensity multiday rainfall events and simulated a 3-day event with a single rain shower of 2 mm on day one, 5 mm on day two, and 2 mm on day three, and 24-hr drying period between showers. All rainfall experiments were performed using the Griffith University Mobile Rainfall Simulator, which is a portable oscillating spray-type rainfall simulator similar to that described by Loch et al. (2001) and detailed by Bullard et al. (2018). The rainfall simulator comprises a water tank with pump and 4 × Veejet 80100 nozzles at a height of 2.5 m, which sweep across the area of interest at a predetermined rate. Average drop diameter is 3–4 mm, and kinetic energies produced by the nozzles are estimated as 29.5 J/m^2, which is similar to that reported for natural rainfall where intensity exceeds 40 mm/hr (Loch et al., 2001; Rosewell, 1986). The rainfall simulator provides a very uniform spatially pattern of intensity with a mean Christiansen Uniformity Coefficient (Christiansen, 1942) of 90.23 ± 1.66, which is well above the minimum acceptable value of 80% (Esteves et al., 2000; Iserloh et al., 2013). A rainfall intensity of 60 mm/hr was achieved using a sweep duration of 0.55 s and wait time of 3 s and is an appropriate approximation of rainfall intensity at the soil collection sites (Connolly et al., 1998). Between showers, the soils were dried at 35 °C and 30% humidity to simulate summer conditions in the semiarid drylands of eastern Australia.

2.3. Soil Surface Roughness Characterization

The small-sized aggregates in the soils used here (<1.4 mm) and cyanobacterial filaments typical of early successional stage CBCs (Campbell, 1979; Garcia-Pichel & Wojciechowski, 2009) necessitated measurement of SSR at a very high resolution to capture change between rainfall applications. Noncontact laser scans (<0.5-mm horizontal and <0.5-mm vertical) have recently been demonstrated as ideal for capturing small-scale physical (Bullard et al., 2018; Zielinski et al., 2014) and biological (O'Brien & McKenna Neuman, 2012; Rodríguez-Caballero et al., 2012) changes at the soil surface, and this approach was adopted for this paper.

Before treatment, and after each rainfall applied, each soil surface was scanned using a Micro-Epsilon ScanCONTROL 2900-100 laser profiler mounted on a computer-controlled, motor-driven traversing frame —detailed methodology is described by Bullard et al. (2018). The scanner was mounted at a height of 24 cm above the soil surface and used to scan an area of the soil 100 × 100 mm at a horizontal and vertical resolution of 78 μm (0.078 mm). To minimize edge effects, the central area of 80 × 80 mm in the center of each scan was extracted for analysis (~1.5 million data points). The laser scan data were postprocessed onto a 0.078 mm grid using MatLab to produce digital elevation models (DEMs) of the soil surface before and after each rain application (t = 0; t = 2; t = 7; t = 9—where the value represents both the total cumulative rainfall amount [mm] and duration in minutes). Although our experiments were conducted in controlled laboratory conditions it proved difficult to produce a perfectly smooth soil surface yet any slight gradient of the soil surface has a substantial effect on the scan introducing a slope trend. Consequently, all the z data were

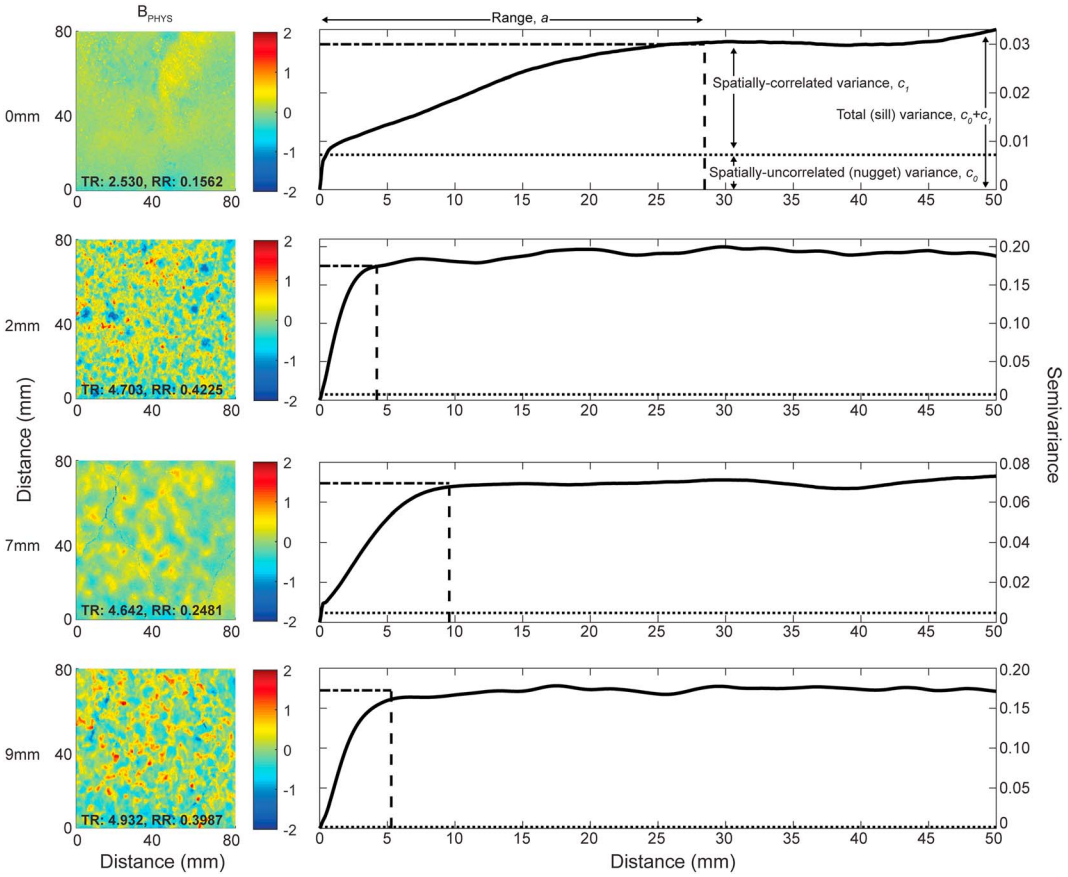

Figure 2. Changes in soil surface roughness for soil B_{PHYS} on exposure to rainfall represented as digital elevation models and empirical semivariograms. Values of a, c_0, c_1, and $c_0 + c_1$ are indicated. Vertical axes differ for each semivariogram.

detrended using a linear model to remove any large-scale oriented roughness, which may create bias in the metrics derived from them (Bullard et al., 2018). Where the laser beam was occluded returning no data for a given point (<0.01% of scan data) the null data point was replaced by an average value calculated from the surrounding eight cells. The mean z value for $t = 0$ was used as the zero level for all digital elevation plots to make it possible to compare the surface after each rain application with the initial conditions.

From the DEM data, a number of aspatial and spatially resolved indices were used to characterize the soil surface roughness. Aspatial metrics look at bulk properties of the soil surface and include topographic range (TR—the difference in height between the lowest and highest detected points in the DEM) and random roughness (RR—the standard deviation in height after eliminating oriented roughness such as slope; Currence & Lovely, 1970). The spatial complexity of SSR was quantified using a semivariogram to which a spherical model was fitted (Corwin et al., 2006). Model results were used to determine four key geostatistically derived indicators which each describe an attribute of SSR; range (a), spatially correlated variance (c_1), nugget variance (c_0) and total (sill) variance ($c_0 + c_1$; Bullard et al., 2018). The range (a) indicates the maximum scale of spatial variation in the data (Atkinson & Tate, 2000) such that larger values of a are associated with larger scales of spatial patterning. Nugget variance (c_0) is spatially uncorrelated variance due to factors such as measurement error or model fitting. Sill variance describes the total amount of spatial variation in the data such that for the same scale, more spatially varied surfaces have higher values of $c_0 + c_1$. There is a strong relationship between $c_0 + c_1$ and RR that highlights the link between the total amount of spatial variation in the data set and the vertical component of roughness (Bullard et al., 2018; Croft et al., 2013). The range a provides a quantitative measure of the horizontal component of roughness variation. Figure 2 shows how changes in surface roughness for different soil states are represented in the DEMs and empirical semivariograms.

Table 2
Summary of SSR and Associated Data for soils A and B With Physical ($_{PHYS}$) and Cyanobacteria ($_{CBC}$) Crusts

Sample	Cumulative rainfall (mm)	Cracks	Ponding	Surface resistance (kg/cm^2)	Infiltration rate (mm/s^1)	TR (mm)	RR (mm)	Range a (mm)	Spatially correlated variance c_1	Nugget variance c_0	Sill variance $c_0 + c_1$	RMSE height (μm)
A_{PHYS}	0			0	0.006	1.25	0.09	34.32	0.01	0.00	0.01	
	2	✓		0.50		5.85	0.31	3.88	0.10	0.00	0.10	6.08
	7	✓	3:00	1.58		9.46	0.20	8.50	0.03	0.01	0.04	2.20
	9	✓		2.30	0.001	6.10	0.23	5.78	0.06	0.00	0.06	0.67
A_{CBC}	0			1.87		1.89	0.13	38.51	0.01	0.01	0.02	0.96
	2			>6		1.71	0.01	49.37	0.03	0.01	0.03	0.98
	7	✓		5.81		3.11	0.15	48.24	0.02	0.01	0.03	0.97
	9	✓		5.92	0.006	2.84	0.15	43.86	0.22	0.01	0.03	0.96
B_{PHYS}	0			0	0.014	2.35	0.16	28.45	0.02	0.01		0.67
	2	✓		0.47		4.70	0.42	4.22	0.18	0.01	0.18	6.11
	7	✓	2:00	0.78		4.64	0.25	9.57	0.06	0.00	0.06	1.41
	9	✓		0.92	0.006	4.93	0.40	5.28	0.17	0.00	0.17	4.29
B_{CBC}	0			2.79		3.14	0.21	17.90	0.03	0.01	0.04	0.92
	2			>6		3.66	0.21	16.74	0.02	0.02	0.04	0.93
	7			5.92		4.59	0.23	14.71	0.03	0.02	0.05	0.90
	9			5.93	0.001	5.06	0.24	15.94	0.02	0.03	0.05	0.89

Note. Surface cracking presence (✓) or absence. Time of ponding following start of rainfall is indicated in minutes:seconds. TR = topographic range; RR = random roughness; RMSE = root-mean-square error. Variogram statistics a, c_1, c_0, $c_0 + c_1$ extracted from the fitting of a spherical model to the variogram data for each soil after each application of rainfall

2.4. Soil and Crust Measurements

Crust strength was measured using resistance to compressive pressure using a Geotester pocket penetrometer with a 5-mm diameter tip 24 hr after each rainfall simulation. Previous studies have demonstrated that crust compressive strength is generally positively related to cyanobacterial biomass (Xie et al., 2007) and a reasonable indicator of the stabilizing effect of both physical and biological crusts in the landscape. Where the crust could not be penetrated using the 5-mm tip, a narrower 2-mm tip was used and force (kg/cm^2) calculated accordingly. Six measurements of resistance were made after each rain application in reserved trays for physical crusts and at one end of the longer trays used to grow the CBCs to avoid affecting the nondestructive measurements.

Steady state infiltration was determined on dry soils both prerainfall and postrainfall simulation for abiotic soils and postrainfall only for the biotic soils. A minidisk infiltrometer was used which allows water to infiltrate while under tension to prevent the filling of macropores (Decagon Devices Inc, 2007; Nciizah & Wakindiki, 2014). Infiltration rate was determined using an extension of the manufacturer's guidance that optimizes results for fine-textured soils (for details see Dohnal et al., 2010).

Net soil loss caused by rainsplash was measured by capturing any sediment that was removed from the tray by rainsplash particle detachment. The soil trays were placed within larger trays (290 × 420 × 60 mm for soils without CBCs; 1,500 × 500 × 60 mm for soils on which biological crusts had been grown); following each rain fall, particles captured within the outer trays were dried, weighed, and net rainsplash loss in grams per square meter calculated to allow comparison between the two tray sizes. This method does not measure total detachment where particles are entrained but redeposited within the tray but does indicate soil loss from a defined area.

3. Results

Prior to rainfall (t = 0), the abiotic soils (A_{PHYS}, B_{PHYS}) were loose and unconsolidated with negligible surface resistance (Table 2). The rainfall-drying sequence led to a successive increase in physical crust strength for both soils but the crust was stronger for soil A_{PHYS}, which has a higher clay and silt content than for sand-

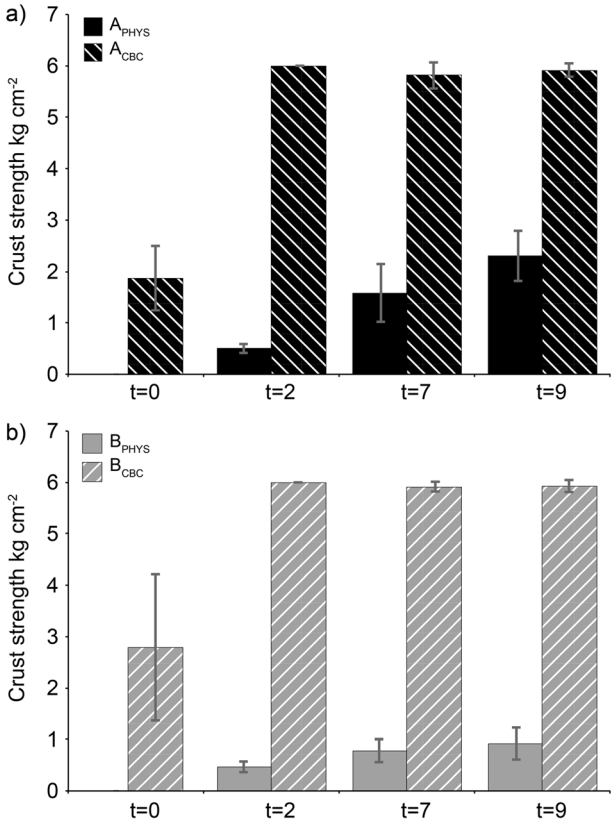

Figure 3. Surface crust strength measurements for (a) soil A and (b) soil B with and without cyanobacteria.

rich B_{PHYS} (Table 1). The soils on which CBCs had been grown had developed a thin biological crust with a stronger crusts developed on the loamy fine sand soil (B_{CBC} = 2.79 kg/cm^2) compared to the sandy loam (A_{CBC} = 1.87 kg/cm^2). Following the first application of rainfall the cyanobacterial crusts on both soils became very resistant reaching the maximum instrument reading of 6 kg/cm^2 at t = 2 and remaining consistently high for the remainder of the experiment (Figure 3).

Pre-experimentation infiltration rates were more than twice as rapid for soil B (0.0138 mm/s) compared to soil A (0.0059 mm/s; Table 2). For both soils infiltration rates were lower following the application of rainfall regardless of whether cyanobacteria were present or not. The infiltration rate for A_{CBC} at t = 9 was only slightly lower than prerainfall at 0.0055 mm/s, but the rate for A_{PHYS} decreased markedly to 0.0008 mm/s. At t = 9 infiltration rate for B_{PHYS} was approximately half that prior to any rainfall. Infiltration at t = 9 for B_{CBC} was very low at 0.0012 mm/s.

Splash erosion rates were substantially higher for the soils with physical only crusts compared to those with cyanobacterial crusts (Figure 4). In all cases, splash erosion was highest during the 5 mm rainfall application.

The occurrence of soil surface cracks and ponding was noted throughout the experiments (Table 2). Cracks appeared on A_{PHYS} and B_{PHYS} as they dried following the first 2 mm of rainfall and persisted to the end of the experiment. The development of a large crack on A_{PHYS} is reflected in the increase in topographic range from 1.25 mm at t = 0, to 5.85 mm at t = 2, to 9.46 mm at t = 7. Surface ponding was observed on the physical soils during the 5-mm rainfall and occurred after 3 min for soil A and 2 min for soil B. No ponding was observed on the two soils with cyanobacterial crusts, but a fine crack developed on A_{CBC} at t = 7 persisting to t = 9.

Both soils were smoothed prior to the application of rainfall and CBC growth. This is reflected in low topographic range (<2 mm for soil A; <3.2 mm for soil B) and random roughness, and high values of a that are associated with a smooth surface and large-scale pattering (Table 2). In both cases SSR was higher at t = 0 for the soils with CBC than those without which reflects the presence of cyanobacteria at the soil surface (visually identified by light green coloring: Belnap et al., 2008; Strong et al., 2013). The application of 2 mm of rain resulted in the development of raindrop impact structures (Bullard et al., 2018) and sieving crusts (Rajot et al., 2003) on A_{PHYS} and B_{PHYS} that can clearly be seen in the photographs in Figures 5 and 6. The sieving crust was best developed on the sandier soil (B_{PHYS}). These structures are characterized in the semivariograms by a substantial increase in values of the sill variance from $c_0 + c_1$ = 0.01 to 0.10 (A_{PHYS}) and 0.02 to 0.18 (B_{PHYS}), which describes increased spatial variation and a decrease in a (from 34.32 to 3.88 A_{PHYS} and 28.45 to 4.22 B_{PHYS}), which is associated with a change from large to small scale patterning. In contrast the t = 2 mm rainfall had much less impact on the SSR of soils with CBCs, which have only minor changes in sill variance (<0.03 alteration). For soil A_{CBC} topographic roughness slightly decreased following 2 mm of rainfall from 1.89 mm (t = 0) to 1.71 (t = 2). For soil B_{CBC} topographic roughness increased slightly from 3.14 (t = 0) to 3.66 (t = 2).

The addition of a further 5-mm rainfall (t = 7) caused a decrease in SSR for the physical soils and a change back to a much smoother surface with large scale patterning (high values of a, low values of $c_0 + c_1$; Table 2). For soil A_{PHYS} sill variance decreased from a high of 0.10 (t = 2) to 0.04 at t = 7 and while the semivariogram regained a similar shape to that of A_{CBC}, the physical soil remained rougher overall (Figure 4). For soil B, SSR for B_{PHYS} decreased and at t = 7 the physical and CBC soils had very similar spatial roughness characteristics.

The final application of 2-mm rainfall (t = 9) resulted in a slight increase to surface patterning and SSR for A_{PHYS} but not as much as that following the first application (t = 2). For B_{PHYS} the final 2 mm of rainfall resulted in the re-establishment of a sieving crust with visible raindrop impact structures and a comcomitant increase

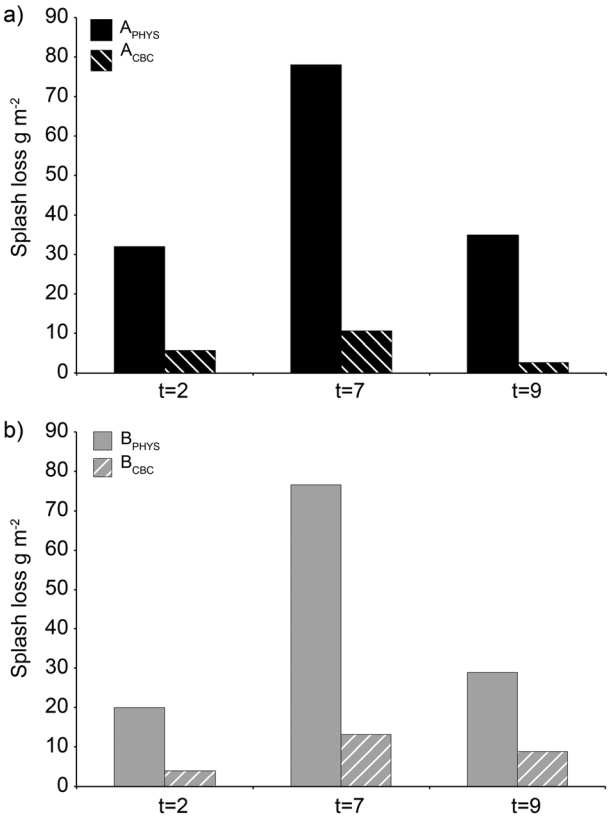

Figure 4. Splash erosion measurements for (a) soil A and (b) soil B with and without cyanobacteria.

in the sill variance and decrease in *a*. Overall, the application of rainfall has a more marked effect on the SSR of the physical soils, which were very responsive to each treatment. The SSR of soils with CBCs was far less responsive to rainfall, and although SSR indicators did vary for each treatment, the absolute variability was substantially lower than for soils without CBCs. The variability of spatial patterning was also greater on the physical soils than on the biotic soils.

4. Discussion

The increase in soil surface resistance to penetration following rainfall on A_{PHYS} and B_{PHYS} suggests raindrop impact caused the development of a physical crust. Successive application of rainfall increased the physical crust strength as would be expected from previous studies (Freebairn et al., 1991; Fan et al., 2008; Feng et al., 2013; Nciizah & Wakindiki, 2014). The physical crusts developed on soil A are stronger than those on soil B. Although the sand-sized aggregates in soil B can be broken down to silt and clay-sized particles (reduction in percent sand from 76% MD to 58% ID: Table 1) the greater crust strength of soil A is likely due to the higher overall proportion of silt-sized material compared to that in soil B as silt-rich, less stable aggregates are more likely to be broken apart by raindrop impact (Fu et al., 2017) and compacted to create a seal or crust.

The biotic soils on which CBCs had been grown had a higher crust strength at $t = 0$ than the physical crusts despite having been dried to $<5\%$ moisture content prior to testing. This sustained resistance of CBCs to penetration even under dry conditions has been previously observed in laboratory (e.g., McKenna Neuman et al., 1996) and field-based studies (e.g., Chamizo et al., 2015). The rapid increase in CBC strength on both soils in response to 2-mm rainfall was sustained for successive rainfall applications. This likely reflects two, not mutually exclusive, processes. First, cyanobacteria respond very rapidly to even small amounts of rainfall (Strong et al., 2013), increasing their biomass, which includes the growth of a network of filaments at the soil surface and the secretion of extracellular polysaccharides, which bind soil particles together (Belnap & Gardner, 1993; Felde et al., 2016; Garcia-Pichel & Wojciechowski, 2009; Mager & Thomas, 2011; Schulten, 1985). A limitation to interpreting our results is that no direct measurement of biomass change in response to rainfall was made for this study. The assumption made is that biomass will have increased in response to rainfall, and this is supported by studies that have found a clear relationship between cyanobacterial biomass and the compressive strength of biotic crusts, particularly where *Microcoleous* spp. and *Phormidium* spp. are present in the soil, as was the case here (Wu et al., 2013; Xie et al., 2007). Second, in natural (field) conditions, CBCs are often associated with depositional physical crusts (Cantón et al., 2003; Lázaro et al., 2008), which have a moderately high crust strength (Casenave & Valentin, 1992). The conditions in which the CBCs were grown for this project are unlikely to have enabled a physical depositional crust to form in conjunction with the CBCs due to the very light hydration regime used. However, any exposed areas of the CBC trays not colonized by cyanobacteria could be expected to form two-layered structural *sieving* crusts (Bullard et al., 2018; Rajot et al., 2003) as observed to have formed on the abiotic soils used here. This type of structural crust has a similar relative strength to depositional crusts (Casenave & Valentin, 1992). Given the substantially higher compressive strength of A_{CBC} and B_{CBC}, and very low standard errors, at all stages compared to that of A_{PHYS} and B_{PHYS}, the cyanobacterial crust is likely to be dominant and of a near uniform and complete cover (see also Figure 1).

The presence of a cyanobacterial crust reduced the susceptibility of the soil to rain splash erosion. This protection is afforded by the same biological components that contribute to CBC crust strength, namely, the combination of cyanobacterial filaments on the soil surface and the chemical binding of particles by polysaccharides both of which increase aggregate stability and reduce water erosion (Eldridge & Greene, 1994; Chamizo, Cantón, Miralles, et al., 2012; Colica et al., 2014), although penetration resistance has not been

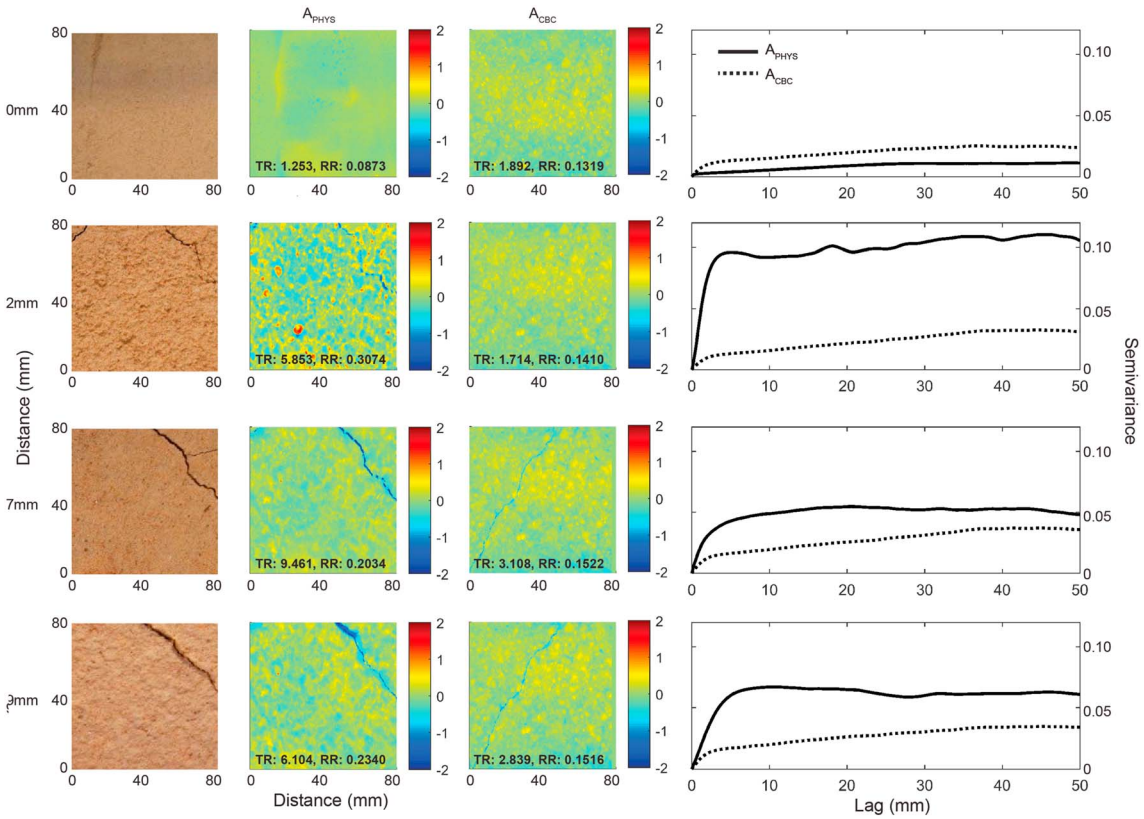

Figure 5. Soil surface roughness characteristics for soil A at $t = 0$ to $t = 9$. (first column) Color photographs of soil surface for A_{PHYS}, (second column) digital elevation models for A_{PHYS}, (third column) digital elevation models for A_{CBC}, and (fourth column) empirical semivariograms for A_{PHYS} and A_{CBC}.

found to be a good indicator of soil detachment response (Chamizo et al., 2015). In this study splash erosion was around 5 times higher at $t = 2$ for both soil A and B and 6–7 times higher at $t = 7$ for the physical crusted soils compared to when a cyanobacterial crust is present. For $t = 9$ splash erosion was 12 times higher for A_{PHYS} compared to A_{CBC} and 3 times higher for B_{PHYS} compared to B_{CBC}. This is comparable to other studies a selection of which is summarized in Table 3 and suggest remarkably similar percentage reductions in soil loss where CBCs are present despite the variability in rainfall duration, intensity, and overall experimental design. Kheirfam et al. (2017) found soil loss was 5 times higher on soils with no CBC compared to those with soils on which CBC had been growing for 15 days. The erosion protection offered by the cyanobacteria increased with the number of days over which the CBC was allowed to develop. The CBCs in this study were grown for 60 days and reduced soil erosion splash loss by 83%–95% for 2-mm rainfall, and 91%–94% for 2 + 5-mm rainfall ($t = 7$), which compares well with Kherifam et al.'s (2017) findings that 60-day-old cyanobacterial crusts reduced soil loss by 99% (Table 3). Chamizo et al. (2015) found that cyanobacterial crust growing on a sandy loam soil only reduced soil losses by 50% compared to CBC on a silty loam where soil loss was reduced by 90%. This study compared a sandy loam with a loamy fine sand and found the CBC growing on the former, with a higher proportion of silts and clays, to provide less protection than the latter which has a higher proportion of sand. The difference in protection against splash erosion is most noticeable for the last rainfall application ($t = 9$) where the reduction in soil loss for A_{CBC} (sandy loam) was only 65% compared with 97% for B_{CBC} (loamy fine sand). This suggests that soil texture plays an important role in determining splash loss susceptibility alongside CBC development. Studies of rainsplash detachment suggest less energy is required to detach fine sand-sized particles (100–200 μm) than those which are coarser or finer than this range (Salles et al., 2000). In addition, splash lengths are longer for fine sands than other sediments (Leguédois et al., 2005). The observation that soils with fine sands at the surface, such as those which have a well-developed sieving crust (i.e., the physical crusted soils) have higher splash erosion losses than those where this type of crust is absent or only covers

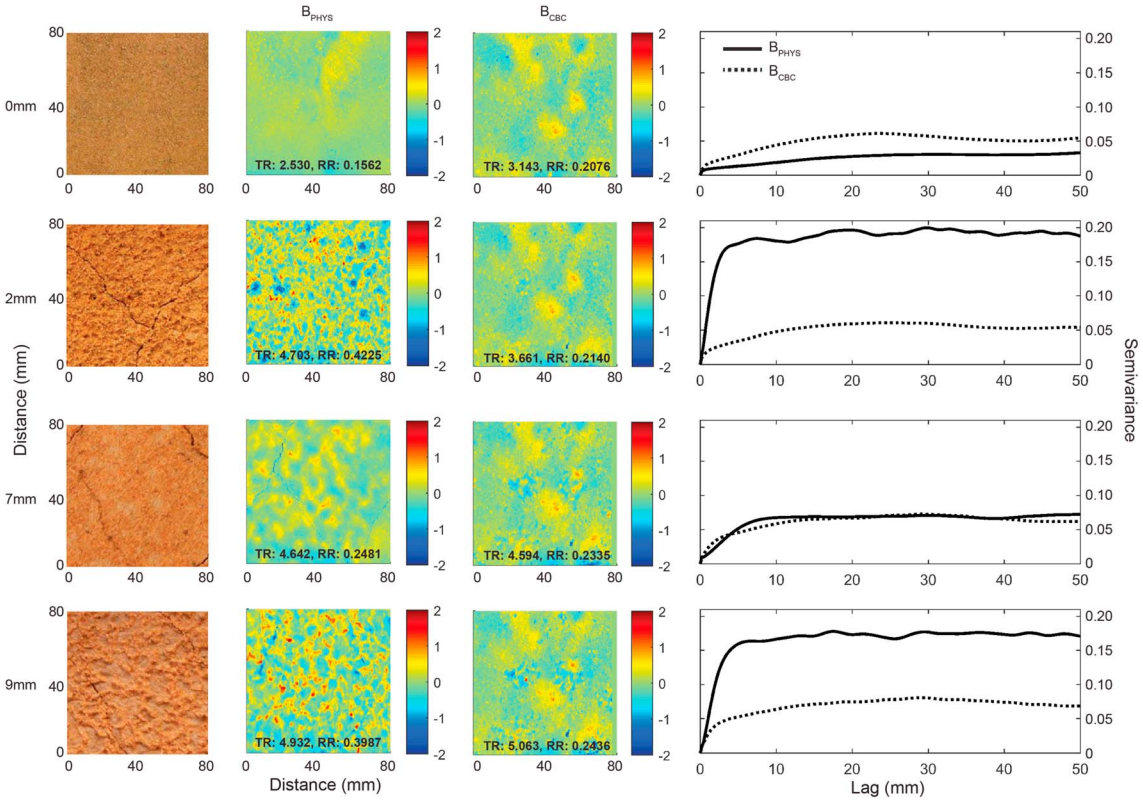

Figure 6. Soil surface roughness characteristics for soil B at $t = 0$ to $t = 9$. (first column) Color photographs of soil surface for B_{PHYS}, (seconnnd column) digital elevation models for B_{PHYS}, (third column) digital elevation models for B_{CBC}, and (fourth column) empirical semivariograms for B_{PHYS} and B_{CBC}.

Table 3
Summary of Selected Studies to Determine the Impact of CBCs on Soil Loss Reduction

Reference	Rainfall		Experiment	Soil type	Percent reduction in soil loss where CBC present
	Duration (min)	Intensity (mm/hr)			
This study	2	60	Laboratory study; see text for details	Sandy loam	93%
				Loamy fine sand	95%
	2 + 5			Sandy loam	91%
				Loamy fine sand	94%
	2 + 5 + 2			Sandy loam	65%
				Loamy fine sand	97%
Eldridge and Greene (1994)	20	45	Laboratory study; natural cryptogam assemblage	Loam clay loam	c. 75%
Hill et al. (2002)	30	43–50	Laboratory study; natural cyanobacteria assemblage	Coarse to fine gravelly clayey sand	79%
				Sandy clay loam	96%
Chamizo et al. (2015)	30	50	Field study; CBC removed by scalping	Sandy loam	50%
				Silty loam	90%
Chamizo et al. (2017)	10–72 mm (four events)	5–47 mm	Field study; natural rainfall events, CBC removed by scalping	Silty loam	84%
Kheirfam et al. (2017)	100	50 mm/hr	Laboratory study; artificial inoculation, grown for 60 days	Silty clay loam	98%

Note. CBC = Cyanobacterial soil crusts.

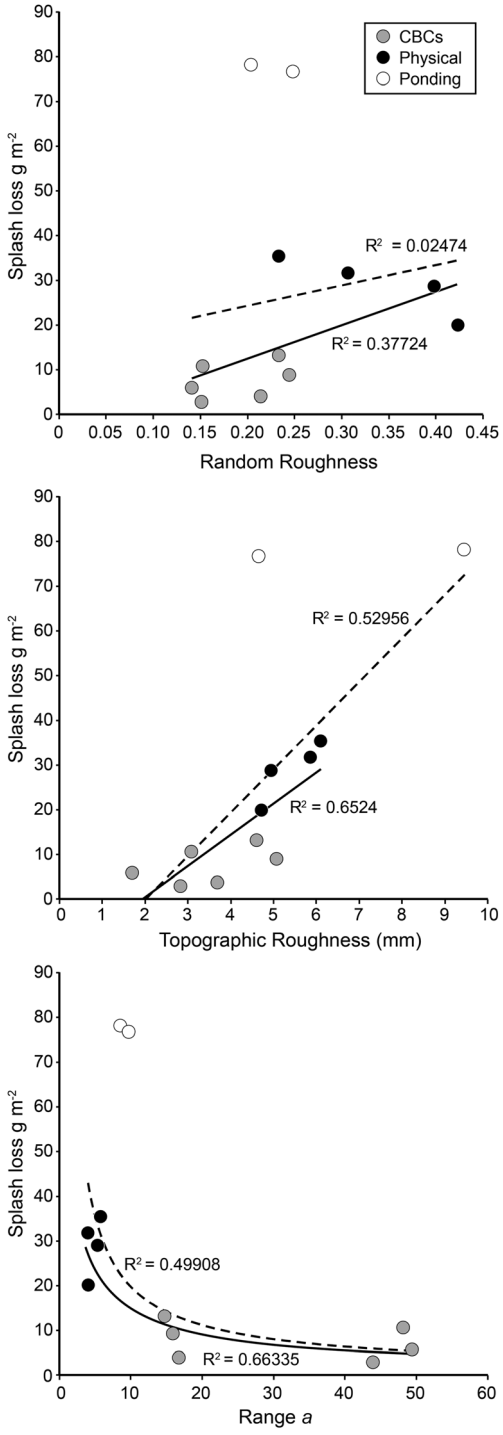

Figure 7. Relationships between splash loss and (a) random roughness, (b) topographic roughness, (c) range *a*. Green filled circles indicate soils with cyanobacteria-dominated biological soil crusts (CBCs), black filled circles indicate soils with physical crusts on which ponding did not occur, and open circles indicate soils with physical crusts on which ponding occurred at $t = 7$. Best fit lines are shown for all data (dashed line) and data excluding points where ponding occurred (solid line)—see text for details.

a very small percentage of the surface accords with these studies. The relative inefficiency of the CBC crust in protecting soil B at $t = 9$ may be due to the higher proportion of surface sand in this soil. In addition small-scape rupturing of crusts may have occurred but this was not directly observed (O'Brien & McKenna Neuman, 2012).

Although it has been suggested that surface smoothing by cyanobacteria can result in higher runoff (e.g., Faist et al., 2017), that is not the case here when compared to the physical crusted soils. Ponding did not occur at any time on A_{CBC} or B_{CBC}; however, it did occur on A_{PHYS} and B_{PHYS} during the 5-mm rainfall application. This is most likely because the presence of cyanobacteria prevented the development of a surface seal but also due to its affect increasing infiltration rates, which can lead to a decrease in runoff (Chamizo, Cantón, Lázaro, et al., 2012; Lázaro et al., 2015). On the sandy loam soil the infiltration rate at the end of the experiment was almost the same for A_{CBC} ($t = 9$) as it was for A_{PHYS} prior to any rainfall ($t = 0$) suggesting soil pore spaces were being maintained. In contrast, on the loamy fine sand infiltration was lower on the soil with cyanobacterial crust (B_{CBC}) at $t = 9$ than for that without (B_{PHYS}) at $t = 9$. This supports Warren's (2001) suggestion that cyanobacteria can reduce infiltration rates on sandy soils by blocking soil pore spaces.

The light cyanobacterial crusts examined here are initially slightly rougher than the abiotic soil surfaces (Figures 4 and 5), but they prevent the soil surface particles from being dislodged or removed by rainfall. CBCs are very resistant to raindrop impact (Lázaro & Mora, 2014) and up to 15 times more resistant to kinetic energy than bare soils (Qin & Zhao, 2011; Zhao et al., 2014). This resistance is demonstrated here by the minimal change in the A_{CBC} and B_{CBC} semivariograms with successive treatments compared with the A_{PHYS} and B_{PHYS} semivariograms, which are highly variable.

Soil surface roughness attributes have been widely demonstrated to affect runoff, infiltration, and soil erosion losses although research suggests the interactions vary with some studies finding a decrease in soil loss with increasing SSR and others an increase in soil loss (Cogo et al., 1984; Ding & Huang, 2017; Gomez & Nearing, 2005; Helming et al., 1998; Römkens et al., 2001). A rougher soil surface might be expected to reduce rainfall energy and cause the ponding of water in depressions both of which decrease splash rate (Govers et al., 2000); however, the spatial resolution, scale, and cause of SSR (e.g., aggregate sizes, tillage, and vegetation) can confound this relationship. Very few studies have attempted to quantify soil surface roughness on soils with cyanobacterial crusts. One of the first, by Rodríguez-Caballero et al. (2012), identified a weak linear relationship between RR and sediment yield for biologically crusted soils in which the greater the roughness, the lower the sediment yield; however, this relationship only explained around one third of the erosion variance. The relationship between RR and splash loss for all soils in this study is shown in Figure 7 and suggests that splash loss might increase with increasing RR, although the relationship is very weak and not statistically significant; there is a much stronger relationship between TR and splash loss suggesting that as TR increases, sediment loss increases.

The findings presented here suggest that sediment loss is higher from rougher surfaces, which is counterintuitive given rougher surfaces would be expected to increase the likelihood of detached particles becoming lodged in depressions and retained within the study area. However, the trapping effectiveness of a rough surface will be dependent not only

on the vertical component of roughness but also on the horizontal component (described by sill variance and range *a*). Typically, as random roughness increases, spatial variation (sill variance) will also increase (Bullard et al., 2018; Croft et al., 2013), which is the case for the data presented here (r^2 = 0.9363; n = 16). High values of RR (and TR) can be associated with both small-scale patterning or with larger-scale patterning (as quantified by *a*) depending on the area of interest. Bullard et al. (2018) found that for very fine soils with small aggregates, such as those tested here, the horizontal (range *a*) component of SSR was determined by raindrop impact which is a driver of splash erosion. When splash loss is plotted against *a* the result is a significant power law relationship in which the larger the scale of spatial patterning, the less splash loss occurs (Figure 7). In each panel of Figure 7 two data points with particularly high splash loss stand out. These are A_{PHYS} t = 7 and B_{PHYS} t = 7, which are the only two measurements associated with soil surface ponding. During the 5 mm rainfall event the development of a surface seal on the soils reduced infiltration and caused water to pond but the very fine scale roughness and low absolute vertical relief meant that rather than the ponding resulting in sediment storage, as might be expected on rougher soils, the depressions filled rapidly resulting in surface flow and a greater loss of soil. If the points where ponding occurred are removed from the data sets in Figure 7, due to representing soil loss via overland flow rather than splash erosion, the relationships between vertical and horizontal roughness components and splash loss are all marginally improved.

At the outset of this paper, it was suggested that during a rain event the SSR of soils without BSCs would be expected to decrease due to aggregate disintegration, whereas the SSR of soils with BSCs might be expected to increase due to organism growth and water absorption. This hypothesis was not borne out by this study as the soils with physical crusts became rougher than those with cyanobacterial crusts during rainfall simulations. The reason for this is likely due to the type of soil used, level of development of the CBC and the rainfall regime that was simulated. As the soils had only very fine aggregates, the absolute reduction of SSR due to disaggregation was small and the primary determinant of SSR, particularly after the 2-mm rainfall applications, was raindrop impact and the microtopography associated with the development of a sieving crust (Bullard et al., 2018). The presence of CBCs before the rainfall treatment made the soil surface rougher than the abiotic soil, but despite being early successional stage, this was sufficient to protect the soil from raindrop impact and erosion, as has been demonstrated elsewhere during inoculation studies (Kheirfam et al., 2017; Sadeghi et al., 2017). The surface roughness of the soils with CBCs did increase very slightly with each treatment (slight increases in RR and TR). This increase is in line with the order of magnitude expected from the swelling of cyanobacterial filaments in response to wetting (Rodríguez-Caballero et al., 2015) or may be due to rainfall-induced growth or motility of filaments which can be very rapid (Campbell, 1979; Rao et al., 2009). The rainfall event simulated here is typical of high frequency, low-magnitude events that occur where these CBCs are naturally found. As such, the rainfall totals were lower than has been used in many other investigations (e.g., Table 3). Working at the same field site from which these soils were collected, Chappell et al. (2007) conducted in situ rainfall simulations and found that in some cases, rainfall did cause a greater increase in surface roughness of soils with BSCs compared with those without; however, the rainfall intensity used was much higher (110 mm/hr for 5 min) than in the experiments reported here.

The results presented here reinforce previous studies highlighting the protective function of cyanobacterial crusts against soil loss by splash erosion. The development of any type of crust has the potential to reduce both water and wind erosion, but some research suggests cyanobacterial crusts are more resistant to erosion than physical crusts (O'Brien & McKenna Neuman, 2012) and that deflation and (Abed et al., 2012) runoff (Sadeghi et al., 2017) are reduced particularly where filamentous cyanobacteria are present at the soil surface. All crusts can be fragile and are vulnerable to rupturing by both natural processes such as saltation bombardment (O'Brien & McKenna Neuman, 2012) or anthropogenic activity such as off-road vehicular activity (Leys & Eldridge, 1998; McLaurin et al., 2011). The protective effect of crusts will potentially last until they are ruptured or reworked by sufficiently high magnitude natural events (e.g., rain or wind storms and flooding).

5. Conclusion

This study examined the response of soil surface roughness to rainfall and differs from previous research in a number of ways. First, the soils used were from an arid region with naturally small aggregates (<1.4 mm) and very low organic matter content. Although the experiments were not conducted in situ, the rainfall conditions simulated were of a typical duration and intensity of high-frequency, low-magnitude events found in

the soil source region and the natural biota in the soils was used to grow the cyanobacterial crusts (rather than artificial inoculation). This study therefore used experimental variables appropriate to deepen understanding of landscape processes, while low-frequency, high-intensity rainfall events can cause dramatic changes in landscapes; the incremental changes driven by high-frequency events are also important and need to be explored. Second, soil surface roughness was quantified at much higher resolution for this study than in many other cases. This was done in order to capture small-scale changes on the soil surface caused by individual particle movements and the presence and growth of cyanobacteria.

Two different soils were tested, and soil texture was found to impact physical crust strength, where the soil with higher clay and silt content was more resistant than that with a higher sand content. In contrast cyanobacterial crust strength prior to rainfall was higher on the sandier soil but there was no difference between CBC strength on the soils in response to rainfall. The cyanobacterial soil crusts were consistently stronger and splash erosion was substantially less than from the physical soil crusts. This was a small study testing only two soil types, and due to a lack of replicates, the interpretation of the results has been largely descriptive rather than statistical. Nevertheless, a comparison of this study with other research suggests that for rainfall events up to ~100 mm total the effectiveness of CBCs in reducing soil loss is typically >80% regardless of rainfall amount and intensity which highlights their importance for landscape stabilization. Under some conditions soil loss reduction is less effective (50%–65%); this may be due to the interaction between the cyanobacteria and soil texture. Future research could usefully compare physical and biological soil crust impacts on a wider range of soils because the impact of cyanobacteria on properties such as infiltration is known to vary with soil texture.

Prior to rainfall treatment, the soils with cyanobacterial crusts had greater SSR than those without. The first and subsequent rainfall treatments caused the physical crusted soils to increase SSR and spatial patterning due to the translocation of particles, soil loss, and the development of raindrop impact craters. Rainfall caused swelling of cyanobacterial filaments but only a slight increase in SSR, and raindrop impact cratering and splash loss were very low on the soils with cyanobacterial crusts. For low rainfall totals and the soils tested here there is no relationship between random roughness and splash erosion, but an increase in splash loss was associated with an increase in topographic roughness and smaller-scale spatial patterning. A useful extension to this work would be to examine SSR dynamics for CBCs over more wetting-drying growth cycles to determine the rate and nature of changes associated with the development of the soil biological community.

Acknowledgments
Many thanks are due to Kyle Barton, Hossein Ghadiri and Grant McTainsh (Griffith University, Australia) for assistance with use of the rainfall simulator and David Elliott (The University of Derby, UK) for cyanobacteria DNA analysis. JEB, CLS and HA were funded by the UK Natural Environment Research Council (NE/K011461/1); AO was funded by Loughborough University. Soil samples obtained from Diamantina Lakes National Park under permit number: WITK15785115 granted by the Queensland Government, Department of Environment and Heritage Protection. Data used in this paper form part of the NE/K011461/1 dataset archived at the UK National Geoscience Data Centre (http://www.bgs.ac.uk/services/ngdc/home.html release date end 2019).

References

Abed, R. M. M., Ramette, A., Hübner, V., De Deckker, P., & de Beer, D. (2012). Microbial diversity of eolian dust sources from saline lake sediments and biological soil crusts in arid southern Australia. *FEMS Microbiology Ecology*, *80*(2), 294–304. https://doi.org/10.1111/j.1574-6941.2011.01289.x

Abrahams, A. D., Li, G., Krishnan, C., & Atkinson, J. F. (2001). A sediment transport equation for interrill overland flow on rough surfaces. *Earth Surface Processes and Landforms*, *26*(13), 1443–1459. https://doi.org/10.1002/esp.286

Agassi, M., Morin, J., & Shainberg, I. (1985). Effect of drop impact energy and water salinity on filtration rates of sodic soils. *Soil Science Society of America Journal*, *49*(1), 186–190. https://doi.org/10.2136/sssaj1985.03615995004900010037x

Antoine, M., Javaux, M., & Bielders, C. (2009). What indicators can capture runoff-relevant connectivity properties of the micro-topography at the plot scale? *Advances in Water Resources*, *32*(8), 1297–1310. https://doi.org/10.1016/j.advwatres.2009.05.006

Assouline, S. (2004). Rainfall-induced soil surface sealing: A critical review of observations, conceptual models and solutions. *Vadose Zone Journal*, *3*, 570–591.

Atkinson, P., & Tate, N. (2000). Spatial scale problems and geostatistical solutions: A review. *The Professional Geographer*, *52*(4), 607–623. https://doi.org/10.1111/0033-0124.00250

Bedaiwy, M. N. A. (2008). Mechanical and hydraulic resistance relations in crust-topped soils. *Catena*, *72*(2), 270–281. https://doi.org/10.1016/j.catena.2007.05.012

Belnap, J. (2006). The potential roles of biological soil crusts in dryland hydrologic cycles. *Hydrological Processes*, *20*(15), 3159–3178. https://doi.org/10.1002/hyp.6325

Belnap, J., & Gardner, J. S. (1993). Soil microstructure in soils of the Colorado plateau: The role of the cyanobacterium *Microcoleus vaginatus*. *Great Basin Naturalist*, *53*, 40–47.

Belnap, J., Phillips, S. L., Witwicki, D. L., & Miller, M. E. (2008). Visually assessing the level of development and soil surface stability of cyanobacterially dominated biological soil crusts. *Journal of Arid Environments*, *72*(7), 1257–1264. https://doi.org/10.1016/j.jaridenv.2008.02.019

Belnap, J., Welter, J. R., Grimm, N. B., Barger, N., & Ludwig, J. A. (2005). Linkages between microbial and hydrologic processes in arid and semiarid watersheds. *Ecology*, *86*(2), 298–307. https://doi.org/10.1890/03-0567

Bradford, J. M., & Huang, L. (1993). Comparison of inter-rill soil loss for laboratory and field procedures. *Soil Technology*, *6*(2), 145–156. https://doi.org/10.1016/0933-3630(93)90003-W

Bullard, J. E., Ockelford, A., Strong, C. L., & Aubault, H. (2018). Impact of multi-day rainfall events on surface roughness and physical crusting of very fine soils. *Geoderma*, *313*, 181–192. https://doi.org/10.1016/j.geoderma.2017.10.038

Cammeraat, L. H. (2002). A review of two strongly contrasting geomorphological systems within the context of scale. *Earth Surface Processes and Landforms*, *27*(11), 1201–1222. https://doi.org/10.1002/esp.421

Campbell, S. E. (1979). Soil stabilization by a prokaryotic desert crust: Implications for Precambrian land biota. *Origins of Life*, *9*(4), 335–348. https://doi.org/10.1007/BF00926826

Cantón, Y., Solé-Benet, A., & Lázaro, R. (2003). Soil–geomorphology relations in gypsiferous materials of the Tabernas desert (Almería, SE Spain). *Geoderma*, *115*(3-4), 193–222. https://doi.org/10.1016/S0016-7061(03)00012-0

Carmi, G., & Berliner, P. (2008). The effect of soil crust on the generation of runoff on small plots in an arid environment. *Catena*, *74*(1), 37–42. https://doi.org/10.1016/j.catena.2008.02.002

Casenave, A., & Valentin, C. (1992). A runoff capability classification system based on surface features criteria in semi-arid areas of West Africa. *Journal of Hydrology*, *130*(1-4), 231–249. https://doi.org/10.1016/0022-1694(92)90112-9

Chamizo, S., Cantón, Y., Lázaro, R., & Domingo, F. (2013). The role of biological soil crusts in soil moisture dynamics in two semiarid ecosystems with contrasting soil textures. *Journal of Hydrology*, *489*, 74–84. https://doi.org/10.1016/j.jhydrol.2013.02.051

Chamizo, S., Cantón, Y., Lázaro, R., Solé-Benet, A., & Domingo, F. (2012). Crust composition and disturbance drive infiltration through biological soil crusts in semiarid ecosystems. *Ecosystems*, *15*(1), 148–161. https://doi.org/10.1007/s10021-011-9499-6

Chamizo, S., Cantón, Y., Miralles, I., & Domingo, F. (2012). Biological soil crust development affects physicochemical characteristics of soil surface in semiarid ecosystems. *Soil Biology and Biochemistry*, *49*, 96–105. https://doi.org/10.1016/j.soilbio.2012.02.017

Chamizo, S., Rodríguez-Caballero, E., Cantón, Y., Asensio, C., & Domingo, F. (2015). Penetration resistance of biological soil crusts and its dynamics after crust removal: Relationships with runoff and soil detachment. *Catena*, *126*, 164–172. https://doi.org/10.1016/j.catena.2014.11.011

Chamizo, S., Rodríguez-Caballero, E., Román, J. R., & Cantón, Y. (2017). Effects of biocrust on soil erosion and organic carbon losses under natural rainfall. *Catena*, *148*, 117–125. https://doi.org/10.1016/j.catena.2016.06.017

Chappell, A., Strong, C., McTainsh, G., & Leys, J. (2007). Detecting induced insitu erodibility of a dust-producing playa in Australia using a bi-directional soil spectral reflectance model. *Remote Sensing of Environment*, *106*(4), 508–524. https://doi.org/10.1016/j.rse.2006.09.009

Chappell, A., Zobeck, T. M., & Brunner, G. (2006). Using bi-directional soil spectral reflectance to model soil surface changes induced by rainfall and wind-tunnel abrasion. *Remote Sensing of Environment*, *102*(3-4), 328–343. https://doi.org/10.1016/j.rse.2006.02.020

Christiansen, J. E. (1942). *Irrigation by sprinkling, California agriculture experiment station bulletin* (Vol. 670, 124 pp.). Berkeley: University of California.

Cogo, N. P., Moldenhauer, W. C., & Foster, G. R. (1984). Soil loss reductions from conservation tillage practices. *Soil Science Society of America Journal*, *48*(2), 368–373. https://doi.org/10.2136/sssaj1984.03615995004800020029x

Colica, G., Li, H., Rossi, F., Li, D. H., Liu, Y. D., & DePhilippis, R. (2014). Microbial secreted exopolysaccharides affect the hydrological behavior of induced biological soil crusts in desert sandy soils. *Soil Biology and Biochemistry*, *68*, 62–70. https://doi.org/10.1016/j.soilbio.2013.09.017

Connolly, R. D., Schirmer, J., & Dunn, P. K. (1998). A daily rainfall disaggregation model. *Agricultural and Forest Meteorology*, *92*(2), 105–117. https://doi.org/10.1016/S0168-1923(98)00088-4

Corwin, D. L., Hopmans, J., & de Rooij, G. H. (2006). From field- to landscape-scale vadose zone processes: Scale issues, modelling and monitoring. *Vadose Zone Journal*, *5*(1), 129–139. https://doi.org/10.2136/vzj2006.0004

Croft, H., Anderson, K., Brazier, R. E., & Kuhn, N. J. (2013). Modeling fine-scale soil surface structure using geostatistics. *Water Resources Research*, *49*, 1858–1870. https://doi.org/10.1002/wrer.20172

Currence, H. D., & Lovely, W. G. (1970). The analysis of soil surface roughness. *Transactions of ASAE*, *13*, 710–714.

Darboux, F., Gascuel-Odoux, C., & Davy, P. (2002). Effect of surface water storage by soil roughness on overland flow generation. *Earth Surface Processes and Landforms*, *27*(3), 223–233. https://doi.org/10.1002/esp.313

Decagon Devices Inc (2007). *Mini ddisk infiltrometer: Use manual version 6*. Pullman, WA: Decagon Devices Inc.

Ding, W., & Huang, C. (2017). Effects of soil surface roughness on interrill erosion processes and sediment particle size distribution. *Geomorphology*, *295*, 801–810. https://doi.org/10.1016/j.geomorph.2017.08.033

Dohnal, M., Dusek, J., & Vogel, T. (2010). Improving hydraulic conductivity estimates from minidisk infiltrometer measurements for soils with wide pore-size distributions. *Soil Science Society of America Journal*, *74*(3), 804–811. https://doi.org/10.2136/sssaj2009.0099

Eldridge, D. J., & Greene, R. S. B. (1994). Assessment of sediment yield by splash erosion on a semiarid soil with varying cryptogam cover. *Journal of Arid Environments*, *26*(3), 221–232. https://doi.org/10.1006/jare.1994.1025

Emerson, W., & Greenland, D. (1990). Soil aggregates—Formation and stability. In M. De Boodt, M. Hayes, & A. Herbillon (Eds.), *Soil Colloids and their Associations in Aggregates* (pp. 485–511). New York: Plenum Press. https://doi.org/10.1007/978-1-4899-2611-1_18

Esteves, M., Planchon, O., Lapetite, J. M., Silvera, N., & Cadet, P. (2000). The "EMIRE" large rainfall simulator: Design and field testing. *Earth Surface Processes and Landforms*, *25*(7), 681–690. https://doi.org/10.1002/1096-9837(200007)25:7<681::AID-ESP124>3.0.CO;2-8

Faist, A. M., Herrick, J. E., Belnap, J., Van Zee, J. W., & Barger, N. N. (2017). Biological soil crust and disturbance controls on surface hydrology in a semi-arid ecosystem. *Ecosphere*, *8*(3), e01691.https://doi.org/10.1002/ecs2.1691

Fan, Y., Lei, T., Shainberg, I., & Cai, Q. (2008). Wetting rate and rain depth effects on crust strength and micromorphology. *Soil Science Society of America Journal*, *72*(6), 1604–1610. https://doi.org/10.2136/sssaj2007.0334

Farres, P. (1978). The role of time and aggregate size in the crusting process. *Earth Surface Processes*, *3*(3), 243–254. https://doi.org/10.1002/esp.3290030304

Felde, V. J. M. N. L., Rossi, F., Colesie, C., Uteau-Puschmann, D., Horn, R., Felix-Henningsen, P., et al. (2016). Pore characteristics in biological soil crusts are independent of extracellular polymeric substances. *Soil Biology and Biochemistry*, *103*, 294–299. https://doi.org/10.1016/j.soilbio.2016.08.029

Feng, G., Sharratt, B., & Vaddella, V. (2013). Windblown soil crust formation under light rainfall in a semiarid region. *Soil and Tillage Research*, *128*, 91–96. https://doi.org/10.1016/j.still.2012.11.004

Ferrenberg, S., Tucker, C. L., & Reed, S. C. (2017). Biological soil crusts: Diminutive communities of potential global importance. *Frontiers in Ecology and the Environment*, *15*(3), 160–167. https://doi.org/10.1002/fee.1469

Freebairn, D. M., Gupta, S. C., & Rawls, W. J. (1991). Influence of aggregate size and micro-relief on development of surface soil crusts. *Soil Science Society of America Journal*, *55*(1), 188–195. https://doi.org/10.2136/sssaj1991.03615995005500010033x

Fu, Y., Li, G.-l., Zheng, T.-h., Li, B.-q., & Zhang, T. (2017). Splash detachment and transport of loess aggregate fragments by raindrop action. *Catena*, *150*, 154–160. https://doi.org/10.1016/j.catena.2016.11.021

Garcia-Pichel, F., & Wojciechowski, M. F. (2009). The evolution of a capacity to build supra-cellular ropes enabled filamentous cyanobacteria to colonise highly erodible substrates. *PLoS One*, *4*(11), e7801. https://doi.org/10.1371/journal.pone.0007801

Gomez, J. A., & Nearing, M. A. (2005). Runoff and sediment losses from rough and smooth soil surfaces in a laboratory experiment. *Catena*, *59*(3), 253–266. https://doi.org/10.1016/j.catena.2004.09.008

Govers, G., Takken, I., & Helming, K. (2000). Soil roughness and overland flow. *Agronomie*, *20*(2), 131–146. https://doi.org/10.1051/agro:2000114

Helming, K., Römkens, M. J. M., & Prasad, S. N. (1998). Surface roughness related processes of runoff and soil loss: a flume study. *Soil Science Society of America Journal*, *62*, 243–250. https://doi.org/10.2136/sssaj1998.03615995006200010031x

Hill, R. D., Nagarkar, S., & Jayawardena, A. W. (2002). Cyanobacterial crust and soil particle detachment: A rain-chamber experiment. *Hydrological Processes*, *16*(15), 2989–2994. https://doi.org/10.1002/hyp.1082

Iserloh, T., Ries, J. B., Arnáez, J., Boix-Fayos, C., Butzen, V., & Cerdà, A. (2013). European small portable rainfall simulators: A comparison of rainfall characteristics. *Catena*, *110*, 100–112. https://doi.org/10.1016/j.catena.2013.05.013

Kamphorst, E. C., Jetten, V., Guérif, J., Pitkänen, J., Iversen, B. V., Douglas, J. R., & Paz, A. (2000). Predicting depressional storage from soil surface roughness. *Soil Science Society of America Journal*, *64*(5), 1749–1758. https://doi.org/10.2136/sssaj2000.6451749x

Kheirfam, H., Sadeghi, S. H., Darki, B. Z., & Honaee, M. (2017). Controlling rainfall-induced soil loss from small experimental plots through inoculation of bacteria and cyanobacteria. *Catena*, *152*, 40–46. https://doi.org/10.1016/j.catena.2017.01.006

Kidron, G. J. (2007). Millimeter-scale microrelief affecting runoff yield over microbiotic crust in the Negev Desert. *Catena*, *70*(2), 266–273. https://doi.org/10.1016/j.catena.2006.08.010

Kidron, G. J., Barinova, S., & Vonshak, A. (2012). The effects of heavy winter rains and rare summer rains on biological soil crusts in the Negev Desert. *Catena*, *95*, 6–11. https://doi.org/10.1016/j.catena.2012.02.021

Kinnell, P. I. A. (2005). Raindrop impact induced erosion processes and prediction: A review. *Hydrological Processes*, *19*(14), 2815–2844. https://doi.org/10.1002/hyp.5788

Kirkby, M. (2002). Modeling the interactions between soil surface properties and water erosion. *Catena*, *46*(2-3), 89–102. https://doi.org/10.1016/S0341-8162(01)00160-6

Lázaro, R., Calvo-Cases, A., Lázaro, A., & Molina, I. (2015). Effective run-off flow length over biological soil crusts on silty loam soils in drylands. *Hydrological Processes*, *29*(11), 2534–2544. https://doi.org/10.1002/hyp.10345

Lázaro, R., Cantón, Y., Solé-Benet, A., Bevan, J., Alexander, R., Sancho, L. G., & Puigdefábregas, J. (2008). The influence of competition between lichen colonization and erosion on the evolution of soil surfaces in the Tabernas badlands SE Spain and its landscape effects. *Geomorphology*, *102*(2), 252–266. https://doi.org/10.1016/j.geomorph.2008.05.005

Lázaro, R., & Mora, J. L. (2014). Sediment content and chemical properties of water runoff on biocrusts in drylands. *Biologia*, *69*(11), 1539–1554. https://doi.org/10.2478/s11756-014-0466-5

Le Bissonais, Y. (1996a). Aggregates stability and assessment of soil crustability and erodibility: I. Theory and methodology. *European Journal of Soil Science*, *47*(4), 425–437. https://doi.org/10.1111/j.1365-2389.1996.tb01843.x

Le Bissonais, Y. (1996b). Soil characteristics and aggregate stability. In M. Agassi (Ed.), *Soil erosion, conservation and rehabilitation* (pp. 41–60). NY: Dekker.

Le Bissonais, Y., Cerdan, O., Lecomte, V., Benkhadra, H., Souchère, V., & Martin, P. (2005). Variability of soil surface characteristics influencing runoff and interrill erosion. *Catena*, *62*(2-3), 111–124. https://doi.org/10.1016/j.catena.2005.05.001

Leguédois, S., Planchon, O., Legout, C., & Le Bissonnais, Y. (2005). Splash projection distance for aggregated soils: Theory and experiment. *Soil Science Society of America Journal*, *69*, 30–37. https://doi.org/10.2136/sssaj2005.0030

Leys, J. F., & Eldridge, D. J. (1998). Influence of cryptogamic crust disturbance to wind erosion on sand and loam rangeland soils. *Earth Surface Processes and Landforms*, *23*(11), 963–974. https://doi.org/10.1002/(SICI)1096-9837(1998110)23:11<963::AID-ESP914>3.0.CO;2-X

Loch, R. J., Robotham, B. G., Zeller, L., Masterman, N., Orange, D. N., Bridge, B. J., et al. (2001). A multi-purpose rainfall simulator for field infiltration and erosion studies. *Australian Journal of Soil Research*, *39*(3), 599–610. https://doi.org/10.1071/SR00039

Luo, J., Zheng, Z. C., Li, T. X., & He, S. Q. (2018). Assessing the impacts of microtopography on soil erosion under simulated rainfall, using a multifractal approach. *Hydrological Processes*, *32*(16), 2543–2556. https://doi.org/10.1002/hyp.13170

Mager, D. M., & Thomas, A. D. (2011). Extracellular polysaccharides from cyanobacterial soil crusts: A review of their role in dryland soil processes. *Journal of Arid Environments*, *75*(2), 91–97. https://doi.org/10.1016/j.jaridenv.2010.10.001

Martin, Y., Valeo, C., & Tait, M. (2008). Centimetre-scale digital representations of terrain and impacts on depression storage. *Catena*, *75*(2), 223–233. https://doi.org/10.1016/j.catena.2008.07.005

Mason, J. A., Greene, R. S. B., & Joeckel, R. M. (2011). Laser diffraction analysis of the disintegration of Aeolian sedimentary aggregates in water. *Catena*, *87*(1), 107–118. https://doi.org/10.1016/j.catena.2011.05.015

Mason, J. A., Jacobs, P. M., Greene, R. S. B., & Nettleton, W. D. (2003). Sedimentary aggregates in the Peoria Loess of Nebraska, USA. *Catena*, *53*(4), 377–397. https://doi.org/10.1016/S0341-8162(03)00073-0

McKenna Neuman, C., Maxwell, C. D., & Boulton, J. W. (1996). Wind transport of sand surfaces crusted with photoautotrophic microorganisms. *Catena*, *27*(3-4), 229–247. https://doi.org/10.1016/0341-8162(96)00023-9

McLaurin, B. T., Goossens, D., & Buck, B. J. (2011). Combining surface mapping and process data to assess, predict and manage dust emissions from natural and disturbed land surfaces. *Geosphere*, *7*(1), 260–275. https://doi.org/10.1130/GES00593.1

McTainsh, G. H., Leys, J. F., & Nickling, W. G. (1999). Wind erodibility of arid lands in the Channel Country of western Queensland, Australia. *Zeitschrift für Geomorphologie Supplementband*, *116*, 113–130.

Morin, J., Karen, R., Benjamini, Y., Ben-Hur, M., & Shainberg, I. (1989). Water infiltration as affected by soil crust and moisture profile. *Soil Science*, *148*(1), 53–59. https://doi.org/10.1097/00010694-198907000-00006

Nciizah, A. D., & Wakindiki, I. I. C. (2014). Rainfall pattern effects on crusting, infiltration and erodibility in some south African soils with various texture and mineralogy. *Water SA*, *40*(1), 57–64. https://doi.org/10.4314/wsa.v40i1.7

O'Brien, P., & McKenna Neuman, C. (2012). A wind tunnel study of particle kinematics during crust rupture and erosion. *Geomorphology*, *173-174*, 149–160. https://doi.org/10.1016/j.geomorph.2012.06.005

Qin, N. Q., & Zhao, Y. G. (2011). Responses of biological soil crust to rain and its relief effect on raindrop kinetic energy. *Chinese Journal of Applied Ecology*, *22*(9), 2259–2264.

Rajot, J. L., Alfaro, S. C., Gomes, L., & Gaudichet, A. (2003). Soil crusting on sandy soils and its influence on wind erosion. *Catena*, *53*(1), 1–16. https://doi.org/10.1016/S0341-8162(02)00201-1

Rao, B., Liu, Y., Wang, W., Hu, C., Dunhai, L., & Lan, S. (2009). Influence of dew on biomass and photosystem II activity of cyanobacterial crusts in the Hopq Desert, Northwest China. *Soil Biology and Biochemistry*, *41*(12), 2387–2393. https://doi.org/10.1016/j.soilbio.2009.06.005

Rayment, G. E., & Higginson, F. R. (1992). *Australian laboratory handbook of soil and water chemical methods*. Melbourne, Australia: Inkata press, Pty Ltd.

Rodríguez-Caballero, E., Aguilar, M. A., Cantón, Y., Chamizo, S., & Aguilar, F. J. (2015). Swelling of biocrusts upon wetting induces changes in surface micro-topography. *Soil Biology and Biochemistry*, *82*, 107–111. https://doi.org/10.1016/j.soilbio.2014.12.010

Rodríguez-Caballero, E., Cantón, Y., Chamizo, S., Afana, A., & Sole-Benet, A. (2012). Effects of biological soil crusts on surface roughness and implications for runoff and erosion. *Geomorphology*, *145-146*, 81–89. https://doi.org/10.1016/j.geomorph.2011.12.042

Rodríguez-Caballero, E., Cantón, Y., Chamizo, S., Lázaro, R., & Escudero, A. (2013). Soil loss and runoff in semiarid ecosystems: A complex interaction between biological soil crusts, micro-topography, and hydrological drivers. *Ecosystems*, *16*(4), 529–546. https://doi.org/10.1007/s10021-012-9626-z

Römkens, M. J., & Wang, J. Y. (1986). Effect of tillage on surface-roughness. *Transactions of ASAE*, *29*(2), 0429–0433. https://doi.org/10.13031/2013.30167

Römkens, M. J. M., Helming, K., & Prasad, S. N. (2001). Soil erosion under different rainfall intensities, surface roughness, and soil water regimes. *Catena*, *46*, 103–123. https://doi.org/10.1016/S0341-8162(01)00161-8

Rosewell, C. J. (1986). Rainfall kinetic energy in eastern Australia. *Journal of Climatology and Applied Meteorology*, *25*(11), 1695–1701. https://doi.org/10.1175/1520-0450(1986)025<1695:RKEIEA>2.0.CO;2

Rossi, F., Potrafka, R. M., Garcia Pichel, F., & De Philippis, R. (2012). The role of the exopolysaccharides in enhancing hydraulic conductivity of biological soil crusts. *Soil Biology and Biochemistry*, *46*, 33–40. https://doi.org/10.1016/j.soilbio.2011.10.016

Sadeghi, S. H., Kheirfam, H., Homaee, M., Darki, B. Z., & Vafakhah, M. (2017). Improving runoff behavior resulting from direct inoculation of soil micro-organisms. *Soil and Tillage Research*, *171*, 35–41. https://doi.org/10.1016/j.still.2017.04.007

Salles, C., Poesen, J., & Govers, G. (2000). Statistical and physical analysis of soil detachment by raindrop impact: Rain erosivity indices and threshold energy. *Water Resources Research*, *36*(9), 2721–2729. https://doi.org/10.1029/2000WR900024

Schulten, J. A. (1985). Soil aggregation by cryptogams of sand prairie. *American Journal of Botany*, *72*, 1657e1661.

Smith, M. W. (2014). Roughness in the earth sciences. *Earth-Science Reviews*, *136*, 202–225. https://doi.org/10.1016/j.earscirev.2014.05.016

Strong, C. L., Bullard, J. E., Burford, M. A., & McTainsh, G. H. (2013). Response of cyanobacterial soil crusts to moisture and nutrient availability. *Catena*, *109*, 195–202. https://doi.org/10.1016/j.catena.2013.03.016

Vermang, J., Norton, L. D., Baetens, J. M., Huang, C., & Cornelis, W. M. (2013). Quantification of soil surface roughness evolution under simulated rainfall. *Transactions of the American Society of Agricultural and Biological Engineers*, *56*(2), 505–514.

Wang, L., Zhang, G., Zhu, L., & Wang, H. (2017). Biocrust wetting induced change in soil surface roughness as influenced by biocrust type, coverage and wetting patterns. *Geoderma*, *306*, 1–9. https://doi.org/10.1016/j.geoderma.2017.06.032

Warren, S. D. (2001). Influence of biological soil crusts on arid land hydrology and soil stability. In J. Belnap & O. L. Lange (Eds.), *Biological Soil Crusts: Structure, Function and Management* (pp. 349–360). Berlin: Springer.

Wu, P. P., Rao, B. Q., Wang, Z. C., Hu, C. X., Shen, Y. W., Liu, Y. D., & Li, D. H. (2013). Succession and contributions to ecosystem function of manmade biotic crusts. *Fresenius Environmental Bulletin*, *22*, 252–260.

Xie, Z., Liu, Y., Hu, C., Chen, L., & Li, D. (2007). Relationships between the biomass of algal crusts in fields and their compressive strength. *Soil Biology and Biochemistry*, *39*(2), 567–572. https://doi.org/10.1016/j.soilbio.2006.09.004

Zhao, Y., Qin, N., Weber, B., & Xu, M. (2014). Response of biological soil crusts to raindrop erosivity and underlying influences in the hilly Loess Plateau region, China. *Biodiversity and Conservation*, *23*(7), 1669–1686. https://doi.org/10.1002/s10531-014-0680-z

Zielinski, M., Sánchez, M., Romero, E., & Atique, A. (2014). Precise observation of soil surface curling. *Geoderma*, *226-227*, 85–93. https://doi.org/10.1016/j.geoderma.2014.02.005

Zobeck, T. M., & Popham, T. W. (1997). Modification of the wind erosion roughness index by rainfall. *Soil and Tillage Research*, *42*(1-2), 47–61. https://doi.org/10.1016/S0167-1987(96)01105-1